ACS Catalysis

Letter

pubs.acs.org/acscatalysis

EPR Spectroscopic Detection of the Elusive Fe^{V}=O Intermediates in Selective Catalytic Oxofunctionalizations of Hydrocarbons Mediated by Biomimetic Ferric Complexes

Oleg Y. Lyakin,[†,‡] Alexandra M. Zima,[†,‡] Denis G. Samsonenko,[†,§] Konstantin P. Bryliakov,[†,‡] and Evgenii P. Talsi*[,†,‡]

[†]Novosibirsk State University, Pirogova 2, Novosibirsk 630090, Russian Federation

[‡]Boreskov Institute of Catalysis, Pr. Lavrentieva 5, Novosibirsk 630090, Russian Federation

[§]Nikolaev Institute of Inorganic Chemistry, Pr. Lavrentieva 3, Novosibirsk 630090, Russian Federation

Supporting Information

ABSTRACT: Herein, we report the EPR spectroscopic study of the bioinspired catalyst systems for selective hydrocarbon oxofunctionalizations based on dinuclear ferric complexes with TPA* and PDP* aminopyridine ligands, hydrogen peroxide, and acetic acid (TPA* = tris(3,5-dimethyl-4-methoxypyridyl-2-methyl)amine, PDP* = bis(3,5-dimethyl-4-methoxypyridyl-2-methyl)-(*S*,*S*)-2,2′-bipyrrolidine). Using very low temperatures, −75 to −85 °C, the extremely unstable and reactive iron−oxygen intermediates, directly reacting with olefins even at −85 °C, have been detected for the first time. Their EPR parameters (g_1 = 2.070−2.071, g_2 = 2.005−2.008, g_3 = 1.956−1.960) were very similar to those of the known oxoiron(V) complex $[(TMC)Fe^{V}{=}O(NC(O)CH_3)]^{+}$ (g_1 = 2.053, g_2 = 2.010, g_3 = 1.971, TMC = 1,4,8,11-tetramethyl-1,4,8,11-tetraazacyclotetradecane). On the basis of EPR and reactivity data, the detected intermediates were assigned to the Fe^{V}=O active oxidizing species of the catalyst systems studied.

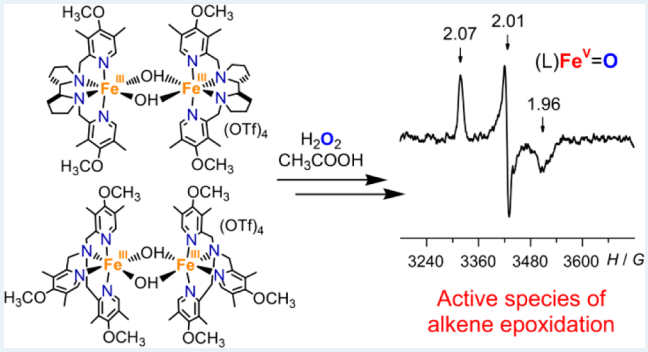

KEYWORDS: *bioinspired catalysis, enantioselective epoxidation, EPR, iron, mechanism*

The selective oxidation of organic molecules is fundamentally important to life.[1a] Although metalloenzyme-catalyzed oxidations often exhibit exquisite substrate specificity as well as regioselectivity and/or stereoselectivity in nature, man-designed synthetic bioinspired, or biomimetic, systems may have broader substrate scope and tunable selectivity, which makes them challenging protagonists of environmentally friendly catalytic chemistry of the near future.[1]

The detection and characterization of the active species of biomimetic catalyst systems, which can also provide important insights into biological pathways, is a hot topic of oxidation chemistry. Catalyst systems based on iron complexes with tetradentate N_4-donor ligands, H_2O_2, and carboxylic acid as an additive have attracted particular attention in the past decade due to high efficiency and selectivity in the preparative oxidations of C−H and C=C groups of various organic molecules.[1−3] The systems **1**−**3**/H_2O_2/CH_3COOH (Chart 1) are among the most extensively studied ones.[2,3] It is generally agreed that species of the type $[(L)Fe^{V}{=}O(OC(O)CH_3)]^{2+}$ are active intermediates of these catalyst systems (L is the corresponding tetradentate ligand).[1e,2b,3c,4] Direct spectroscopic evidence for the putative $(L)Fe^{V}(O)(OH)$ oxidant was obtained by Costas, Cronin, and co-workers from variable-temperature electrospray mass spectrometric experiments in studies of the catalyst system **4**/H_2O_2 (Chart 1).[4] However, the active species of the catalyst systems **1**−**3**/H_2O_2/CH_3COOH have not been unambiguously identified so far.

Previously, we have observed by EPR very unstable and reactive intermediates **1a**−**3a** in the catalyst systems **1**−**3**/H_2O_2/CH_3COOH at −70 to −80 °C and assigned them to the $[(L)Fe^{V}{=}O(OC(O)CH_3)]^{2+}$ species.[3c,5] It should be noted that the EPR parameters of **1a**−**3a** (g_1 = 2.7, g_2 = 2.4, g_3 = 1.5−1.7, see entries 3−5 of Table 1) drastically differed from those of known Fe^{V}=O species (Table 1, entries 1, 2),[6] and were close to those of low-spin ferric complexes. Relying on these data and on the results of DFT calculations, Wang et al. hypothesized that **1a**−**3a** were ferric−peracetate complexes Fe^{III}−$OOC(O)CH_3$ rather than iron(V)−oxo complexes.[7]

In 2014, Oloo et al. reported the detection of the intermediate **X** (g_1 = 2.58, g_2 = 2.38, and g_3 = 1.72) in the catalyst system **1***/H_2O_2/CH_3COOH in acetonitrile at −40 °C.[8] In contrast to complex **1** bearing unsubstituted TPA ligand, the TPA* ligand of **1*** contains donor substituents at

Received: January 27, 2015
Revised: March 19, 2015
Published: March 23, 2015

DOI: 10.1021/acscatal.5b00169
ACS Catal. 2015, 5, 2702−2707

Chart 1. Structures of Aminopyridine Iron Complexes

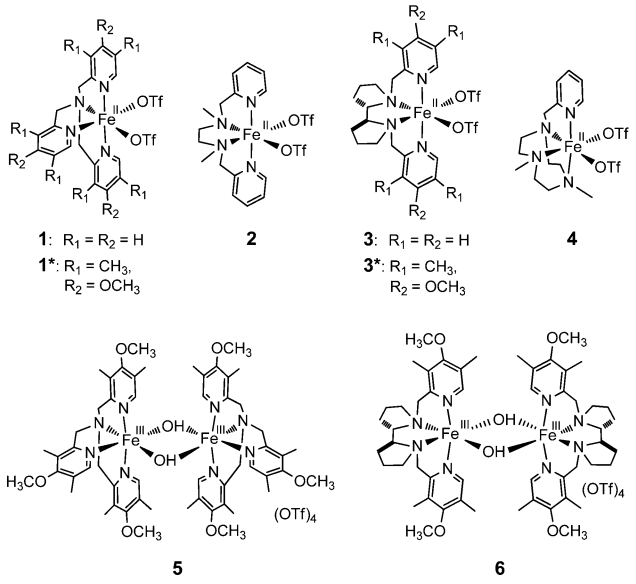

the pyridine rings (Chart 1). By a combination of EPR, Mössbauer, resonance Raman, and ESI-MS methods, **X** was identified as a low-spin acylperoxoiron(III) species $[(TPA^*)Fe^{III}(\kappa^2\text{-}OOC(O)CH_3)]^{2+}$.[8] The rate of decay of complex **X** at −40 °C was unaffected by the presence of cyclooctene, 1-octene or 2-heptene in the reaction solution, ruling out the assignment of **X** to the actual oxygen-transferring species.

So, two important problems remain unresolved: (1) detection of the true oxidizing species of the catalyst system **1***/H_2O_2/CH_3COOH and (2) identification of the intermediates **1a**−**3a**.

In this contribution, we report EPR spectroscopic studies of the catalyst systems **5**/H_2O_2/CH_3COOH and **6**/H_2O_2/CH_3COOH (Chart 1). The dinuclear ferric complexes **5** and **6**[9] were used as the precursors to the active sites, instead of mononuclear ferrous complexes **1*** and **3***, because **1*** and **3*** immediately convert into **5** and **6** just after the addition of H_2O_2 (see below). Using low temperatures (−75 to −85 °C), the extremely unstable and reactive iron−oxygen intermediates **5a** and **6a** have been detected by EPR spectroscopy in the systems **5**,**6**/H_2O_2/CH_3COOH and assigned to the oxoiron(V) intermediates on the basis of their reactivity toward electron-donating alkenes and close similarity of their EPR spectra to those of the known oxoiron(V) species.

The starting dinuclear complex **5** is EPR silent. Just after the addition of 50 equiv of CH_3COOH to the 0.05 M solution of **5** in CH_2Cl_2/CH_3CN = 1.2:1 (by volume) mixture at room temperature and freezing the sample at −196 °C, the EPR signal of a new ferric complex with proposed structure $[(TPA^*)Fe^{III}(\kappa^2\text{-}OC(O)CH_3)]^{2+}$ ($\mathbf{X_5}$) is observed (Figure 1A). This complex displays resonances at g_1 = 2.58, g_2 = 2.38, and g_3 = 1.72. We note that related complexes $[(TPA)Fe^{III}(acac)]^{2+}$ and $[(5\text{-}Me_3TPA)Fe^{III}(acac)]^{2+}$ (Hacac = acetylacetone) show very similar EPR spectra (g_1 = 2.57, g_2 = 2.35, and g_3 = 1.71).[10a] The EPR spectrum of $\mathbf{X_5}$ disappears with the half-life time of $\tau_{1/2}$ = 2 min at room temperature. Besides the resonances of $\mathbf{X_5}$, the EPR spectrum of Figure 1A exhibits the intense resonances at g = 5.6 and 4.3 from stable unidentified high-spin (S = 5/2) ferric species.

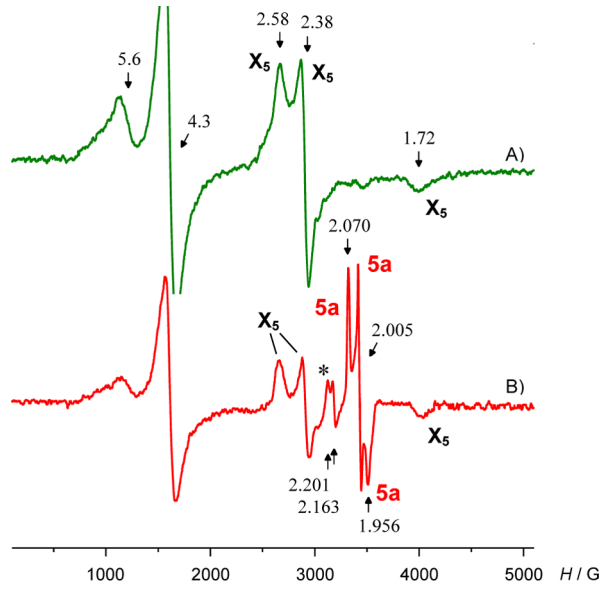

Figure 1. EPR spectra (−196 °C) of the sample (A) **5**/CH_3COOH ([CH_3COOH]/[**5**] = 50, [**5**] = 0.05 M) frozen 1 min after mixing the reagents at room temperature in a 1.2:1 CH_2Cl_2/CH_3CN mixture, and the sample (B) **5**/H_2O_2/CH_3COOH ([**5**]:[H_2O_2]:[CH_3COOH] = 1:6:20, [**5**] = 0.02 M) frozen 1.5 min after mixing the reagents at −80 °C in a 1.8:1 CH_2Cl_2/CH_3CN mixture.

The EPR spectrum (−196 °C) of the sample **5**/H_2O_2/CH_3COOH = 1:6:20 recorded 1.5 min after mixing the reagents at −80 °C exhibits three groups of resonances attributed to the low-spin (S = 1/2) iron complexes (Figure

Table 1. EPR Spectroscopic Data for S = 1/2 Iron Species Formed in the Catalyst Systems Based on Iron Complexes with N_4-donor Tetradentate Ligands

no.	compound	g_1	g_2	g_3	ref
1	$[(TMC)Fe^{V}{=}O(NC(O)CH_3)]^{+}$	2.053	2.010	1.971	6a
2	$[(TAML)Fe^{V}{=}O]^{-}$	1.99	1.97	1.74	6b
3	$[(TPA)Fe^{V}{=}O(OC(O)CH_3)]^{2+}$ (**1a**)	2.71	2.42	1.53	5
4	$[(BPMEN)Fe^{V}{=}O(OC(O)CH_3)]^{2+}$ (**2a**)	2.69	2.42	1.70	5
5	$[((S,S)\text{-}PDP)Fe^{V}{=}O(OC(O)CH_3)]^{2+}$ (**3a**)	2.66	2.42	1.71	3c
6	$[(TPA^*)Fe^{V}{=}O(OC(O)CH_3)]^{2+}$ (**5a**)	2.070	2.005	1.956	this work
7	$[((S,S)\text{-}PDP^*)Fe^{V}{=}O(OC(O)CH_3)]^{2+}$ (**6a**)	2.071	2.008	1.960	this work
8	$[(TPA^*)Fe^{III}(\kappa^2\text{-}OC(O)CH_3)]^{2+}$ ($\mathbf{X_5}$)	2.58	2.38	1.72	this work
9	$[((S,S)\text{-}PDP^*)Fe^{III}(\kappa^2\text{-}OC(O)CH_3)]^{2+}$ ($\mathbf{X_6}$)	2.54	2.41	1.79	this work

TMC − tetramethylcyclam, TAML − macrocyclic tetraamide ligand.

DOI: 10.1021/acscatal.5b00169
ACS Catal. 2015, 5, 2702−2707

Table 2. Oxidation of Cyclohexene with H_2O_2 Catalyzed by Mononuclear and Dinuclear Non-Heme Iron Complexes[a]

entry	catalyst	CH_3COOH (equiv)[b]	cyclohexene oxide[c]	2-cyclohexen-1-one[c]	2-cyclohexen-1-ol[c]	selectivity (%)[d]
1	**1***	–	27	59	52	20
2		10	61	38	31	47
3		100	64	23	19	60
4	**5**	–	23	37	43	22
5		10	62	24	22	57
6		100	67	13	11	74
7		500	72	5	8	85
8	**3***	–	78	36	42	50
9		10	93	23	26	65
10		100	91	20	22	68
11	**6**	–	31	25	31	36
12		10	96	13	18	76
13		100	96	12	12	80
14		500	95	4	5	91

[a] H_2O_2 was delivered by syringe pump over 25 min at room temperature, and 5 extra minutes of stirring were allowed before subjecting the solution to GC analysis. [Fe]:[H_2O_2]:[C_6H_{10}] = 1:10:300. [Fe] = 2.7×10^{-3} M. Observed yields of 1,2-cyclohexanediol were <1%. [b] Relative to mole of iron. [c] Product yield (%) expressed in moles of product per mole of H_2O_2. [d] Selectivity toward epoxidation.

1B). In addition to resonances of residual $\mathbf{X}_5$, the weak resonances at $g_1 = 2.201$ and $g_2 = 2.163$ (marked with asterisk in Figure 1) that can be assigned to complex $[(TPA^*)Fe^{III}–OOH(S)]^{2+}$ (S = CH_3CN, CH_3COOH or H_2O) are observed.[5b,10b,11] A rhombic spectrum $g_1 = 2.070$, $g_2 = 2.005$, $g_3 = 1.956$ belongs to a new species **5a**. The latter is much less temperature-stable ($\tau_{1/2}$ = 5 min at −85 °C, Figure S1, Supporting Information) as compared to intermediate **X**.[8] The evaluated maximum concentration of **5a** approaches about 2–3% of the total iron concentration. The half-life time of **5a** is comparable to that for **3a** ($\tau_{1/2}$ = 7 min at −85 °C)[3b] and **1a** ($\tau_{1/2}$ = 7 min at −70 °C).[5a] The addition of CH_3COOH is necessary for the detection of **5a**. The sample **5**/H_2O_2 containing no acetic acid displayed no EPR signals in the range g = 1.5–3.

The catalyst systems **1***/H_2O_2/CH_3COOH and **5**/H_2O_2/CH_3COOH display very similar activity and selectivity toward the epoxidation of cyclohexene at room temperature (Table 2), suggesting that the same active species might operate in these systems. Apparently, the first 0.5 equiv of H_2O_2 rapidly convert the mononuclear iron(II) complex **1*** into the dimeric iron(III) counterpart,[12] which further eventually generates the active species **5a**.

To directly assess the reactivity of **5a** toward alkene epoxidation, the rates of decay of **5a** in the absence and in the presence of various alkenes were compared. It was found that the addition of relatively small amounts of cyclohexene or *cis*-β-methylstyrene ([alkene]/[Fe] = 0.5) to the sample **5**/H_2O_2/CH_3COOH = 1:6:20 ([**5**] = 0.02 M) results in the decrease of the half-life time of **5a** from $\tau_{1/2}$ = 5 min to $\tau_{1/2}$ < 0.5 min at −85 °C, whereas electron-deficient alkenes (1-acetyl-1-cyclohexene and cyclohexene-1-carbonitrile with an [alkene]/[Fe] ratio up to 10) do not visibly affect the decay rate of **5a**. In the presence of 1-octene as a substrate, a pseudo-first-order rate constant versus amount of added 1-octene was measured. A linear correlation was observed, giving a second-order rate constant $k_2 = 3.2 \times 10^{-2}$ M^{-1} s^{-1} (Figure S17, Supporting Information). Hence, **5a** is highly reactive toward electron-rich alkenes even at −85 °C.

The g-values of **5a** drastically differ from those of intermediates **1a**–**3a** (Table 1). Apparently, this is caused by a different electronic nature of the ligands associated with the presence of electron-donating substituents at the pyridine rings of **5**. To verify this assumption, we have undertaken the search for the intermediate similar to **5a** in a structurally related catalyst system **6**/H_2O_2/CH_3COOH (Chart 1).

It was found that EPR spectrum (−196 °C) recorded just after the addition of 20 equiv of CH_3COOH to the solution of **6** in CH_2Cl_2/CH_3CN = 1.8:1 at room temperature exhibits a rhombic EPR spectrum of a new complex $\mathbf{X}_6$ (Figure 2A, Table 1). $\mathbf{X}_6$ is relatively stable and can be observed even after 30 min of storing the sample at room temperature. As in the previous case, $\mathbf{X}_6$ can be assigned to the low-spin (S = 1/2) ferric complex $[((S,S)\text{-PDP}^*)Fe^{III}(\kappa^2\text{-OC(O)CH}_3)]^{2+}$. After the addition of 6 equiv of H_2O_2 to the sample of Figure 2A at −75 °C and mixing the reagents during 1 min, EPR resonances of a new intermediate **6a** appear (Figure 2B). The simulated EPR spectra of $\mathbf{X}_6$ and **6a** are in good agreement with the experimental ones (Figure S2, Supporting Information). The g-values of **6a** ($g_1 = 2.071$, $g_2 = 2.008$, $g_3 = 1.960$) are very close to those of **5a** ($g_1 = 2.070$, $g_2 = 2.005$, $g_3 = 1.956$). The half-life of

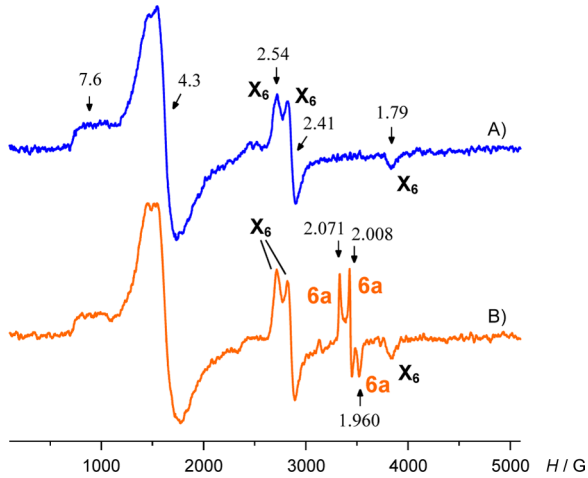

Figure 2. EPR spectra (1.8:1 CH_2Cl_2/CH_3CN, −196 °C) (A) of the sample **6**/CH_3COOH ([CH_3COOH]/[**6**] = 20, [**6**] = 0.02 M) frozen 1 min after mixing the reagents at room temperature and (B) frozen after addition of 6 equiv of H_2O_2 to the sample in "A" at −75 °C and mixing the reagents during 1 min.

DOI: 10.1021/acscatal.5b00169
ACS Catal. 2015, 5, 2702–2707

6a ($\tau_{1/2}$ = 4 min at −85 °C and 2 min at −80 °C, Figures S3 and S4, Supporting Information) is rather close to that for **5a** ($\tau_{1/2}$ = 5 min at −80 °C). The evaluated maximum concentration of **6a** did not exceed 1% of the total iron concentration.

The catalytic properties of the systems **6**/H_2O_2/CH_3COOH and **3***/H_2O_2/CH_3COOH in cyclohexene epoxidation at room temperature are presented in Table 2. It is worth noting that in the presence of acetic acid, dinuclear complex **6** demonstrates even a little better selectivity toward epoxidation than its mononuclear counterpart **3***. Similar catalytic behaviors of complexes **3*** and **6** in the presence of CH_3COOH imply that the same active species is likely to operate in catalyst systems **3***/H_2O_2/CH_3COOH and **6**/H_2O_2/CH_3COOH. The overall yields of cyclohexene oxygenated products >100% as well as the 2-cyclohexen-1-ol/2-cyclohexen-1-one ratio of ca. 1 were found to be unaffected by the addition of triphenylphosphine after the completion of the reaction.[13] Apparently, the 2-cyclohexen-1-peroxyl radicals (formed via trapping O_2 by the initially generated 2-cyclohexen-1-yl radicals) rapidly convert into the corresponding ketone and alcohol in the reaction mixture before subjecting to GC. The amounts of 2-cyclohexen-1-ol and 2-cyclohexen-1-one formed in the course of oxidation dropped upon increasing the amount of acetic acid, thus demonstrating that the latter promotes the major (metal-oxo-mediated) pathway to the epoxide. Notably, much higher epoxide selectivity (up to 99%) was achieved with 10 times larger amount of H_2O_2 ([Fe]:[H_2O_2]:[C_6H_{10}] = 1:102:100; Table S1, Supporting Information) with respect to those observed under conditions where cyclohexene was in a large excess ([Fe]:[H_2O_2]:[C_6H_{10}] = 1:10:300; Table 2). Because the amount of O_2 in the reaction mixture is independent of the catalytic conditions applied, the obtained result corroborates that the allylic oxidation products come from oxygen via a radical mechanism, whereas the epoxide arises from H_2O_2 in the course of a metal-oxo-mediated reaction.

To evaluate the reactivity of **6a** toward alkenes, the sample (**6**/H_2O_2/CH_3COOH = 1:6:20, [**6**] = 0.02 M) containing preliminary generated **6a** was prepared. An alkene was added to this sample at −90 °C within 1 min, and decay of **6a** was monitored at −85 °C. Although in the absence of alkene or in the presence of 1-acetyl-1-cyclohexene and cyclohexene-1-carbonitrile, **6a** decays with $\tau_{1/2}$ = 4 min at −85 °C, the EPR resonances of **6a** disappeared within <0.5 min in the presence of cyclohexene, *cis*-*β*-methylstyrene, and 1-octene at the same temperature ([alkene]/[Fe] = 0.5), demonstrating the direct reactivity of **6a** toward electron-rich alkenes. Catalytic properties of complexes **5** and **6** in 1-octene and *cis*-*β*-methylstyrene oxidations with H_2O_2 are presented in Tables S2 and S3 (Supporting Information), the epoxides being the major oxygenated products. As for cyclohexene oxidation, the epoxide yields and selectivities were found to strongly depend on the amount of added acetic acid. In the absence of the latter, noticeable amounts of 1-octene allylic oxidation products were observed.

Both **5a** and **6a** are electrophilic oxidants. To quantify the products of interaction of **5a** and **6a** with cyclohexene, catalytic oxidation experiments at −85 °C were performed. Both 4.5 and 5.3 TN cyclohexene oxide were obtained 15 min after the reaction onset with catalysts **5** and **6**, respectively (TN = moles of product per mole of Fe, for details see Supporting Information). The total amount of other cyclohexene oxidation products was <1% with respect to the epoxide. Thus, the true active species **5a** and **6a** oxidize cyclohexene even at −85 °C, demonstrating >99% epoxide selectivity.

The half-life times of **5a** and **6a** are rather close to those for **1a**−**3a**. The reactivity of **5a** and **6a** resembles that of **2a**, which epoxidizes cyclohexene at −70 °C.[5a] One can assume that **5a**, **6a**, and **1a**−**3a** are chemically similar intermediates. However, the EPR spectra of **5a** and **6a** indicate a relatively small *g*-tensor anisotropy ($g_{max} - g_{min}$ = 0.1) and sharp resonances ($\Delta H_{1/2}$ = 15−40 G), whereas **1a**−**3a** display highly anisotropic EPR spectra ($g_{max} - g_{min}$ = 1.0−1.2) with much broader resonances ($\Delta H_{1/2}$ = 100−350 G) (Table 1). Apparently, the smaller *g*-tensor anisotropy of **5a** and **6a** is caused by the presence of electron-donating substituents at the pyridine rings but has no connection with the dimeric nature of the starting complexes. Indeed, intermediate **1a** with $g_{max} - g_{min}$ = 1.2 can be generated in the reaction of H_2O_2/CH_3COOH with the in situ prepared dinuclear complex with $(TPA)_2Fe^{III}_2(\mu\text{-}O)$ core (Figure S5D, Supporting Information) in just the same way as starting from the parent mononuclear complex $[(TPA)Fe^{II}(CH_3CN)_2](ClO_4)_2$.[5b]

The main objection against the assignment of **1a**−**3a** to the oxoiron(V) species was the great difference of their *g*-tensors from those of known Fe^{V}=O species.[7] In the case of **5a** and **6a**, the *g*-values and line widths are very similar to those of spectroscopically well-characterized oxoiron complex $[(TMC)Fe^{V}{=}O(NC(O)CH_3)]^+$ (Table 1). The great difference in the EPR spectra of **5a**, **6a** and of the putative oxoiron(V) species **1a**−**3a** implies that electronic structures of those intermediates significantly differ. Indeed, it is well-known that paramagnetic metal complexes demonstrate larger *g*-tensor anisotropy and broader EPR resonances than organic radicals, owing to the occurrence of relatively low-lying excited states and stronger spin−orbit coupling.[14]

It is not counterintuitive that the stronger ligand field induced by aminopyridine ligands bearing powerful electron donors (like in complexes **5** and **6**) may increase the distance between the energies of molecular orbitals, thus reducing the *g*-tensor anisotropy. On the other hand, one can expect that iron complexes with the unpaired spin mainly resting at the metal should display broader resonances and larger *g*-tensor anisotropy than complexes with the unpaired spin mostly delocalized over the ligand. As an example, the EPR parameters of complex with proposed structure $[(TBP_8Cz^{+\bullet})Fe^{IV}{=}O]$ (g_1 =2.09, g_2 = 2.05, g_3 = 2.02 with $g_{max} - g_{min}$ = 0.07; antiferromagnetic coupling between Fe^{IV}=O (S = 1) and $TBP_8Cz^{+\bullet}$ (S = 1/2) is suggested) drastically differ from those of S = 1/2 complex $[(TBP_8Cz)Fe^{III}(Py)]$: g_1 = 2.39, g_2 = 2.20, g_3 = 1.90 with $g_{max} - g_{min}$ = 0.49 (TBP_8Cz = octakis(4-*tert*-butylphenyl)corrolazinato).[15] It is also worth mentioning that antiferromagnetic coupling between Fe^{IV}=O (S = 1) and a ligand cation radical (S = 1/2) is typical for compounds I of heme enzymes, for example, CYP119, the thermophilic cytochrome P450 from *Sulfolobus acidocaldarius*. The reaction of ferric CYP119 with an excess of *m*-chloroperbenzoic acid produces S = 1/2 CYP119 compound I with EPR parameters g_1 = 2.00, g_2 = 1.96, g_3 = 1.86.[16] Very recently, complex $[(Me_3tacn)Fe^{III}(Cl\text{-}acac)Cl]^+$ (Me_3tacn =1,4,7-trimethyl-1,4,7-triazacyclononane, Cl-acac =3-chloro-acetylacetonate) has been used for the oxidation of hydrocarbons with oxone, including cyclohexane, propane, and ethane. ESI-MS, EPR and UV−vis spectroscopy, ^{18}O labeling experiments and DFT studies pointed to $[(Me_3tacn)Fe^{IV}{=}O(\{Cl\text{-}acac\}^{+\bullet})]^{2+}$ as the catalytically active species.[17] EPR parameters of this complex (g_1 =

DOI: 10.1021/acscatal.5b00169
ACS Catal. 2015, 5, 2702−2707

1.97, g_2 = 1.93, g_3 = 1.91) are rather close to those of CYP119 compound I.

With the above reservations in mind, it seems reasonable to assign the intermediates **5a** and **6a** to species of the type $[(L^{+\bullet})Fe^{IV}{=}O(OC(O)CH_3)]^{2+}$. We believe that the presence of strong electron donors in the structures of **5a** and **6a** may favor the intramolecular redistribution of electron density, leading to the reduction of iron to the formal +4 oxidation state, the positive charge being spread over the substituted aromatic rings in structures of the type $[(L^{+\bullet})Fe^{IV}{=}O(OC(O)CH_3)]^{2+}$. In these structures, the unpaired spin is mostly delocalized over the organic ligand framework, thus accounting for the observed low *g*-tensor anisotropy. On the contrary, this scenario is unlikely for intermediates **1a**−**3a** due to the lack of electron density at their unsubstituted pyridine rings. One can expect that the effect of electron-withdrawing substituents on the electronic structure of the high-valent iron−oxygen intermediates should be opposite to the effect of electron-donating substituents, the electron acceptors favoring the formation of intermediates $[(L)Fe^{V}{=}O(OC(O)CH_3)]^{2+}$ with high *g*-tensor anisotropy. In full agreement with this prediction, treating the complex $[((S,S)\text{-PDP-Cl})Fe^{II}(OTf)_2]$,[1e] containing Cl substituents at the *para*-position of the pyridine rings, with CH_3COOH (10 equiv) and H_2O_2 (3 equiv) at −80 °C resulted in the formation of a very unstable iron−oxygen intermediate **3a-Cl** ($\tau_{1/2}$ = 5 min at −80 °C) exhibiting rhombic EPR spectrum g_1 = 2.63, g_2 = 2.41, g_3 = 1.72 (Figure S7, Supporting Information), very similar to that of the unsubstituted species $[((S,S)\text{-PDP})Fe^{V}{=}O(OC(O)CH_3)]^{2+}$ (**3a**, Table 1).

We conclude that **5a**, **6a**, and $[(TMC)Fe^{V}{=}O(NC(O)CH_3)]^{+}$ may be better represented as $(L^{+\bullet})Fe^{IV}{=}O$ rather than $(L)Fe^{V}{=}O$. However, we have used notation $(L)Fe^{V}{=}O$ for intermediates **5a**, **6a** and $[(TMC)Fe^{V}{=}O(NC(O)CH_3)]^{+}$ (Table 1), because further studies are needed to verify their $(L^{+\bullet})Fe^{IV}{=}O$ formulation. The obtained data clearly show that active iron−oxygen intermediates with EPR parameters close to those of known $Fe^{V}{=}O$ species can be trapped in the bioinspired catalyst systems for chemo- and stereoselective oxidation of organic substrates with hydrogen peroxide. On the basis of the EPR spectroscopic and catalytic data obtained in this work, we have proposed the mechanism of alkene epoxidation by the catalyst systems studied (Scheme 1). At the initial stage, dimeric iron complexes reversibly transform into monomeric ferric-acetate complexes ($\mathbf{X_5}$, $\mathbf{X_6}$) observed by EPR even at room temperature. The proposed equilibrium reaction of dimeric iron complexes in Scheme 1 is in accordance with the observed saturation behavior of the concentration of the active species versus the amount of CH_3COOH (Figure S8, Supporting Information). Subsequent interaction of $\mathbf{X_5}$, $\mathbf{X_6}$ with H_2O_2, followed by heterolytic O−O bond cleavage with removal of a water molecule,[2b,3c] generates the active species **5a** and **6a** that directly epoxidize alkenes even at −85 °C.

In summary, this contribution reports on the EPR spectroscopic detection of the extremely unstable iron−oxygen intermediates in catalyst systems based on dinuclear aminopyridine ferric complexes bearing electron-donating substituents, H_2O_2 and acetic acid. The detected intermediates **5a** and **6a** are highly reactive toward electron-rich alkenes even at −85 °C, yielding cyclohexene oxide with >99% selectivity. They exhibit rhombic EPR spectra with *g*-tensor values very similar to those of known *S* = 1/2 oxoferryl complexes. Studies of the catalyst systems based on aminopyridine iron complexes with various electron-donating and electron-withdrawing substituents at the pyridine rings are planned to collect a broader library of EPR data on iron−oxygen species active toward the oxidation of olefins and alkanes.

Scheme 1. Proposed Mechanism of Alkene Epoxidation by Catalyst Systems 5(6)/H_2O_2/CH_3COOH

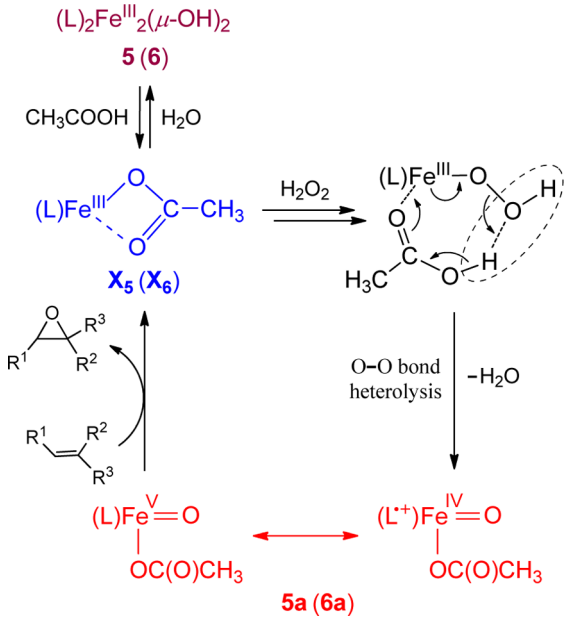

■ ASSOCIATED CONTENT

Supporting Information

The following files are available free of charge on the ACS Publications website at DOI: 10.1021/acscatal.5b00169.

Experimental details, data on the catalytic alkene oxidations, EPR and ^{1}H NMR spectra, X-ray data for **6** (PDF)

Crytallographic information file (CIF).

CCDC 1020311 (complex **6**) contains the supplementary crystallographic data for this paper. These data can be obtained free of charge from the Cambridge Crystallographic Data Centre via www.ccdc.cam.ac.uk/data_request/cif and from the authors.

■ AUTHOR INFORMATION

Corresponding Author

*E-mail: talsi@catalysis.ru.

Notes

The authors declare no competing financial interest.

■ ACKNOWLEDGMENTS

Financial support from the Russian Scientific Foundation (Grant No. 14-13-00158) is gratefully acknowledged. We thank Mr. M.V. Shahkov for the GC-MS measurements.

■ REFERENCES

(1) (a) Que, L., Jr.; Tolman, W. B. *Nature* **2008**, *455*, 333−340. (b) Company, A.; Gómez, L.; Fontrodona, X.; Ribas, X.; Costas, M. *Chem. - Eur. J.* **2008**, *14*, 5727−5731. (c) Wu, M.; Miao, C.-X.; Wang, S.; Hu, X.; Xia, C.; Kühn, F. E.; Sun, W. *Adv. Synth. Catal.* **2011**, *353*, 3014−3022. (d) Wang, B.; Wang, S.; Xia, C.; Sun, W. *Chem. - Eur. J.* **2012**, *18*, 7332−7335. (e) Cussó, O.; Garcia-Bosch, I.; Ribas, X.; Lloret-Fillol, J.; Costas, M. *J. Am. Chem. Soc.* **2013**, *135*, 14871−14878.

DOI: 10.1021/acscatal.5b00169
ACS Catal. 2015, 5, 2702−2707

(f) McDonald, A. R.; Que, L., Jr. *Coord. Chem. Rev.* **2013**, *257*, 414−428. (g) Wang, X.; Miao, C.; Wang, S.; Xia, C.; Sun, W. *ChemCatChem* **2013**, *5*, 2489−2494. (h) Kwon, E.; Cho, K.-B.; Hong, S.; Nam, W. *Chem. Commun.* **2014**, *50*, 5572−5575. (i) Bryliakov, K. P.; Talsi, E. P. *Coord. Chem. Rev.* **2014**, *276*, 73−96.

(2) (a) White, M. C.; Doyle, A. G.; Jacobsen, E. N. *J. Am. Chem. Soc.* **2001**, *123*, 7194−7195. (b) Mas-Ballesté, R.; Que, L., Jr. *J. Am. Chem. Soc.* **2007**, *129*, 15964−15972.

(3) (a) Chen, M. S.; White, M. C. *Science* **2007**, *318*, 783−787. (b) Chen, M. S.; White, M. C. *Science* **2010**, *327*, 566−571. (c) Lyakin, O. Y.; Ottenbacher, R. V.; Bryliakov, K. P.; Talsi, E. P. *ACS Catal.* **2012**, *2*, 1196−1202.

(4) Prat, I.; Mathieson, J. S.; Güell, M.; Ribas, X.; Luis, J. M.; Cronin, L.; Costas, M. *Nat. Chem.* **2011**, *3*, 788−793.

(5) (a) Lyakin, O. Y.; Bryliakov, K. P.; Britovsek, G. J. P.; Talsi, E. P. *J. Am. Chem. Soc.* **2009**, *131*, 10798−10799. (b) Lyakin, O. Y.; Bryliakov, K. P.; Talsi, E. P. *Inorg. Chem.* **2011**, *50*, 5526−5538.

(6) (a) Van Heuvelen, K. M.; Fiedler, A. T.; Shan, X.; De Hont, R. F.; Meier, K. K.; Bominaar, E. L.; Münck, E.; Que, L., Jr. *Proc. Natl. Acad. Sci. U.S.A.* **2012**, *109*, 11933−11938. (b) De Oliveira, F. T.; Chanda, A.; Banerjee, D.; Shan, X.; Mondal, S.; Que, L., Jr.; Bominaar, E. L.; Münck, E.; Collins, T. J. *Science* **2007**, *315*, 835−838.

(7) Wang, Y.; Janardanan, D.; Usharani, D.; Han, K.; Que, L., Jr.; Shaik, S. *ACS Catal.* **2013**, *3*, 1334−1341.

(8) Oloo, W. N.; Meier, K. K.; Wang, Y.; Shaik, S.; Münck, E.; Que, L., Jr. *Nat. Commun.* **2014**, *5*, Article no. 3046.

(9) X-ray data and the molecular structure of complex **6** are presented in the Supporting Information (CCDC 1020311).

(10) (a) Zang, Y.; Kim, J.; Dong, Y.; Wilkinson, E. C.; Appelman, E. H.; Que, L., Jr. *J. Am. Chem. Soc.* **1997**, *119*, 4197−4205. (b) Kim, C.; Chen, K.; Que, L., Jr. *J. Am. Chem. Soc.* **1997**, *119*, 5964−5965.

(11) The third resonance of $[(TPA^*)Fe^{III}–OOH(S)]^{2+}$ at $g_3 = 1.96$ is masked by that of **5a** (Figure 1B).

(12) (a) Chen, K.; Que, L., Jr. *J. Am. Chem. Soc.* **2001**, *123*, 6327−6337. (b) Chen, K.; Costas, M.; Kim, J.; Tipton, A. K.; Que, L., Jr. *J. Am. Chem. Soc.* **2002**, *124*, 3026−3035.

(13) Shul'pin, G. B. *Mini-Rev. Org. Chem.* **2009**, *6*, 95−104.

(14) (a) Pake, G. E. In *Paramagnetic Resonance: an Introductory Monograph*; Pines, D., Ed.; W. A. Benjamin: New York, 1962; pp 55−62. (b) Weil, J. A.; Bolton, J. R. *Electron Paramagnetic Resonance. Elementary Theory and Practical Applications*, 2nd ed.; John Wiley & Sons, Inc.: Hoboken, NJ, 2007; pp 85−117.

(15) McGown, A. J.; Kerber, W. D.; Fujii, H.; Goldberg, D. P. *J. Am. Chem. Soc.* **2009**, *131*, 8040−8048.

(16) Rittle, J.; Green, M. T. *Science* **2010**, *330*, 933−937.

(17) Tse, C.-W.; Chow, T. W.-S.; Guo, Z.; Lee, H. K.; Huang, J.-S.; Che, C.-M. *Angew. Chem., Int. Ed.* **2014**, *53*, 798−803.

DOI: 10.1021/acscatal.5b00169
ACS Catal. 2015, 5, 2702−2707